Isı Bilimi ve Tekniği Dergisi, 44, 1, 227-243, 2024
J. of Thermal Science and Technology

ISSN 1300-3615
e-ISSN 2667-7725
https://doi.org/10.47480/isibted.1494499

EXPLORING THE IMPACT OF GEOMETRIC PARAMETERS ON HEAT TRANSFER AND FLUID FLOW CHARACTERISTICS IN CROSS-TRIANGULAR GROOVED CHANNELS: A COMPUTATIONAL STUDY

Yeliz ALNAK
Sivas Cumhuriyet University, Technology Fac., Manufacturing Eng. Dept., 58140, Sivas, Türkiye
ytas@cumhuriyet.edu.tr, ORCID: 0000-0003-4383-3806

(Geliş Tarihi: 15.02.2024, Kabul Tarihi: 06.04.2024)

Abstract: In this study, the impact of geometric parameters of rectangular baffles with varying location angles and heights is investigated on the heat transfer and fluid flow characteristics of cross-triangular grooved channels. Computational methods are employed to explore these effects, utilizing the Ansys-Fluent program to solve the Navier-Stokes and energy equations, incorporating the k-ε turbulence model for numerical simulations. The inlet temperature of the air, serving as the working fluid, is set at 293 K, while the wall surface temperature of the lower triangular grooved channel remains fixed at 373 K. Rectangular baffles are tested with angles of 30°, 60°, and 90°, and heights of 0.25H, 0.5H, and 0.75H, respectively. The numerical results show good agreement with a 3.53% deviation compared to existing empirical data in the literature. The obtained findings are presented in terms of mean Nusselt (Nu_m) number, fluid temperature, and Performance Evaluation Criterion (PEC) number variations taking into consideration of pressure drop for each rectangular baffle angle and height. Additionally, contour distributions of temperature and velocity are evaluated for different Reynolds numbers (Re) and arrangements of rectangular baffles. It has been determined that the Nu number value increases by 197.56% at a 90° angle and 0.75H height, compared to the 0.25H baffle height at Re=6000. Furthermore, at Re=1000, the PEC number is 84.50% higher with a baffle height of 0.25H and a baffle angle of 30° compared to the condition with a 90° angle.
Keywords: Cross-triangular grooved channels, rectangular baffles, Heat transfer, Computational fluid dynamics, Navier-Stokes equations

ÇAPRAZ ÜÇGEN YİVLİ KANALLARDA GEOMETRİK PARAMETRELERİN ISI TRANSFERİ VE AKIŞKAN AKIŞ ÖZELLİKLERİ ÜZERİNDEKİ ETKİSİNİN ARAŞTIRILMASI: HESAPLAMALI BİR ÇALIŞMA

Özet: Bu çalışmada, konum açıları ve yükseklikleri değişen dikdörtgen engellerin geometrik parametrelerinin çapraz üçgen oluklu kanalların ısı transferi ve akışkan akışı özellikleri üzerindeki etkisi araştırılmaktadır. Bu etkileri keşfetmek için hesaplamalı yöntemler kullanılmış olup; Ansys-Fluent programı kullanılarak Navier-Stokes ve enerji denklemleri çözülmüş, sayısal simülasyonlar için k-ε türbülans modeli dahil edilmiştir. Çalışma akışkanı olarak kullanılan havanın giriş sıcaklığı 293 K iken, üçgen oluklu alt kanalın duvar yüzey sıcaklığı sabit 373 K olarak belirlenmiştir. Dikdörtgen engeller sırasıyla 30°, 60° ve 90° açılarında ve 0,25H, 0,5H ve 0.75H yüksekliklerinde test edilmiştir. Sayısal sonuçlar, literatürde mevcut olan deneysel verilere göre %3,53 sapma ile iyi bir uyum göstermektedir. Elde edilen bulgular, her bir dikdörtgen engel açısı ve yüksekliği için ortalama Nusselt (Nu_m) sayısı, akışkan sıcaklığı ve basınç düşüşünü dikkate alan Performans Değerlendirme Kriteri (PEC) sayısı değişimleri açısından sunulmaktadır. Ayrıca, farklı Reynolds sayıları (Re) ve dikdörtgen engellerin düzenlemeleri için sıcaklık ve hız konturu dağılımları değerlendirilmektedir. Re=6000'de 0,25H engel yüksekliğine göre Nu sayısı değerinin 90° açı ve 0,75H yükseklikte %197,56 arttığı belirlenmiştir. Ayrıca, Re=1000'de, 0,25H engel yüksekliği ve 30° açısında, 90° açıdaki durumla karşılaştırıldığında PEC sayısı %84,50 daha yüksektir.
Anahtar Kelimeler: Çapraz-üçgen oluklu kanallar, Dikdörtgen engeller, ısı transferi, Hesaplamalı akışkanlar dinamiği, Navier-Stokes denklemleri

INTRODUCTION

Heat exchangers play a crucial role in transferring heat from a hot fluid to a cold fluid, finding extensive applications across various industries including heating and cooling systems, chemical manufacturing, oil refining, electrical power generation, and other engineering sectors. Among the different types of heat exchangers, plate heat exchangers are particularly popular due to their compact design, cost-effectiveness, simplicity, and high efficiency. These heat exchangers are continuously evolving and improving, adapting to meet the increasing demands of diverse industries (Liang et. al., 2019).

The parallel plate channel structure represents one of the most common and straightforward configurations of plate heat exchangers. However, its performance is relatively low, prompting many researchers to seek improvements. Scott and Lobato (2003) and Zhang (2005) have made strides in enhancing heat and mass transfer in plate heat exchangers by refining a cross-grooved sinusoidal and triangular channel structure. Their approach involves combining numerous corrugated layers within a plate heat exchanger to create flow channels, with adjacent channels angled specifically to form flow ducts and facilitate fluid separation. This arrangement results in a cross-grooved plate with robust mechanical endurance. Aslan et al. (2023) experimentally and numerically evaluated the friction factor, convection heat transfer and field compliance factor properties of pipe bundles with smooth and offset rows. The Reynolds number was changed from 989 to 6352 and the Pr number was kept at 0.70. It was found that offset orders lead to a larger Nu number and friction factor values compared to smooth arrangement. Notably, at low Reynolds numbers, internal flow becomes turbulent due to the widening feature upon contact in grooved ducts, leading to a notably high coefficient of heat transfer (Zang., 2016).

Researchers have conducted extensive experimental and theoretical investigations aimed at improving the heat transfer performance of cross-grooved channels. Liu and Niu and Niu (2015) examined the impact of aspect ratio and apex angle on the thermal-hydraulic performance of a cross-grooved duct, highlighting the significant influence of the apex angle on the duct's properties. Krishnan et al. (2021) empirically evaluated the effects of corrugation pattern, corrugation angle, plate length, and depth-to-pitch ratio on the thermal-hydraulic performance of grooved flow ducts, emphasizing the importance of groove angle and depth-to-pitch ratio on heat transfer and pressure drop. Saha et al. (2020) investigated the cross-grooved performance of plate heat exchangers across corrugation angle ranges, observing an increase in pressure drop per unit length with an increase in corrugation angle. Guo-Guo-Yan et al. (2005) conducted numerical and experimental analyses on sinusoidal cross-grooved heat exchangers, concluding that a steady-state laminar model is suitable for a specified Reynolds number range, with a slight deviation between computational and empirical results. Zhang et al. (2014, 2005, 2005) studied heat and mass transfer, as well as fluid flow, in cross-grooved triangular ducts for membrane-based exchangers, deriving correlation equations for friction factors, Sherwood numbers, and Reynolds numbers. Li et al. (2015) investigated heat and mass transfer enhancements in cross-grooved membrane exchanger ducts by varying apex angles, finding that larger apex angles resulted in higher Nusselt and Sherwood numbers. Muley and Manglik (1999) analyzed the thermal-hydraulic characteristics of grooved-plate channels with different plate configurations, reporting significantly higher heat transfer compared to flat-plate ducts under equivalent pumping power conditions, considering Reynolds number, chevron angle, and surface area enlargement factor. Zimmerer et al. (2002) studied the wavelength, groove shape, and inclination angle of heat exchangers for local heat and mass transfer and pressure losses. Ajeel et al. (2019) investigated the thermal and hydraulic properties of trapezoidal-grooved ducts using SiO_2-water nanofluid, observing substantial enhancements in Nusselt number with an increase in height-to-width ratio. In another study, Ajeel et al. (2019) explored heat transfer enhancement in grooved channels of semi-circle, trapezoidal, and straight shapes using alumina oxide-water nanofluid, finding the highest enhancement in trapezoidal grooved ducts. Furthermore, Ajeel et al. (2019) empirically evaluated semi-circle-grooved and trapezoidal-grooved ducts using SiO_2-water nanofluid, demonstrating significant improvements in heat transfer rate and pressure drop compared to straight channels.

Baffles serve as effective means to augment heat transfer area, alter the primary flow direction, and enhance flow irregularity and heat transfer. However, there have been relatively few studies utilizing baffles. Li and Gao (2017) examined heat transfer characteristics in cross-grooved triangular ducts employing delta-shaped baffles. They observed a significant increase in pressure drop and a 2.1 to 4.3 times increase in Nusselt number when the baffle height equaled the trough height. Saim et al. (2013) conducted numerical investigations on heat transfer and turbulent flow along ducts with inclined baffles, noting improved friction factor and heat transfer with inclined baffles. Alnak (2020) numerically studied heat transfer, pressure drop, and thermohydraulic performance of cross-grooved triangular ducts with rectangular baffles at different settlement angles. Results showed a 52.8% higher mean Nusselt number for ducts with a 90° angle

baffle compared to those with a 60° angle baffle at Re=6000. Feng et al. (2022) numerically analyzed the impact of trapezoidal baffles on flow and heat transfer properties of cross-grooved triangular ducts. They found Nusselt and friction factors of ducts with trapezoidal baffles to be 1.7 and 3.5 times higher, respectively, than those without baffles, leading to a 30% increase in Performance Evaluation Criterion (PEC) value. Li et al. (2022) investigated the influence of baffle position and apex angle on heat and flow characteristics of cross-corrugated triangular ducts. They introduced trapezoidal baffles to enhance heat transfer, finding that the PEC value for ducts with a specific baffle position at a 120° apex angle could be lower than that without baffles. Liang et al. (2019) conducted computational work using an SST k-ε model to examine six different baffle configurations' effects on temperature patterns and distribution in cross-grooved triangular ducts. They found that compared to ducts without baffles, Nusselt numbers increased by 1.5 to 1.6 times for certain baffle configurations, resulting in a 13% increase in heat transfer efficiency under the same fan power.

The corrugated channels used in the study are employed in the design of plate heat exchangers, which are frequently exerted in heat transfer applications and are formed by combining many thin metal plates. In the reviewed literature, the heat transfer and flow characteristics of baffle setups, spacing, and apex angles in corrugation troughs of cross-grooved channels have been extensively studied. In this study, unlike the studies in the literature, the effects of rectangular baffle angles and heights at the top section of cross-triangular grooved ducts were investigated regarding heat transfer, flow structure, and performance evaluation criterion (PEC) number taking into consideration of pressure drop. Rectangular baffles were positioned at the upper section of the grooved duct at varying angles and heights. Computational research utilized the Ansys-Fluent software program with the k-ε turbulence model to solve steady, three-dimensional equations of energy and Navier-Stokes. The inlet air temperature was set at 293 K, and the fixed surface temperature of the lower triangular grooved ducts was 373 K. Parameters such as Reynolds number and baffle placement angles and heights were varied. The Reynolds number range investigated was 1000-6000, with baffle placement angles of 30°, 60°, and 90°, and heights of 0.25H, 0.5H, and 0.75H. However, in the case of a baffle height of 0.75H when using an angle of 30º, the baffle protrudes from the duct, so the baffle height of 0.75H could not have been analyzed at 30º. Computational results were compared with empirical and computational findings from existing literature, showing agreement. Outcome variables included fluid velocity, temperature, mean Nusselt number (Nu), and performance evaluation criterion (PEC) number along the midpoint of the upper grooved duct section. Additionally, fluid exit temperature variations were assessed for each baffle angle and height, compared to the non-baffle case. Contour distributions of fluid velocity, temperature along the cross-grooved triangular duct were evaluated for various baffle angles and heights at Reynolds numbers of 1000 and 6000.

COMPUTATIONAL METHOD

In this study, numerical solutions for flow and heat transfer were conducted using a 3D, steady-state turbulence model based on the k-ε model within the Ansys-Fluent program. The investigation focused on a cross-triangular grooved triangular channel with various angle and height configurations of rectangular baffles. Convergence criteria were set at 10^-6 and 10^-7 for the energy and momentum equations, respectively. The heat transfer and flow structure analysis for the cross-triangular grooved triangular duct with rectangular baffle placement angles and heights involved solving partial differential equations derived from conservation equations of time-averaged mass, momentum, and energy for turbulent flow. Besides, since irregular flow fluctuations will occur in the channel due to the presence of baffles and grooves in the study, the study was modeled as turbulent, and the k-ε model was used as the turbulence model. However, accurate modeling of turbulence is essential in heat transfer simulations. Direct numerical simulation of turbulent flows is very difficult and time consuming. There are various turbulence models used in numerical modeling. Besides, among turbulence models, the k-ε turbulence model, which is a semi-empirical model, is widely used due to its economy and acceptable accuracy in many flow events. In one of the studies on impinging jets, Wang and Mujumdar (2005) tested several k-ε turbulence models with low Re numbers for turbulent jets. They found that the models were able to determine the general shape of the Nu number distribution and that the models applied better in heated areas for large jet-to-plate distances. In their study, they determined that the k-ε turbulence model showed a good performance in determining the heat transfer properties of impinging jets when compared to standard high Re number models. In addition, compared to other turbulence models (Yıldızeli et. al., 2023), they determined that the k-ε turbulence model is suitable because it reduces kinetic energy production and approaches the required result in the heated zone. Accordingly, taking into account the results obtained from studies in the literature (Karabulut., 2023, Karabulut., 2023, Karabulut and Alnak., 2023), the standard k-ε turbulence model was used in the numerical calculations in this study.

These analyses were carried out under steady-state conditions with no body forces present (Flunet., 2003, Karabulut and Alnak., 2020):
Continuity equation

$$\frac{\partial \bar{u}}{\partial x}+\frac{\partial \bar{v}}{\partial y}+\frac{\partial \bar{w}}{\partial z}=0 \quad (1)$$

Momentum equation:

x momentum equation:

$$\left[\bar{u}\frac{\partial \bar{u}}{\partial x}+\frac{\partial \overline{(u')^2}}{\partial x}\right]+\left[\bar{v}\frac{\partial \bar{u}}{\partial y}+\frac{\partial \overline{(u'v')}}{\partial y}\right]+\left[\overline{w}\frac{\partial \bar{u}}{\partial z}+\frac{\partial \overline{u'w'}}{\partial z}\right]= -\frac{1}{\rho}\frac{\partial \bar{p}}{\partial x}+\nu\left(\frac{\partial^2 \bar{u}}{\partial x^2}+\frac{\partial^2 \bar{u}}{\partial y^2}+\frac{\partial^2 \bar{u}}{\partial z^2}\right) \quad (2.1)$$

y momentum equation:

$$\left[\bar{u}\frac{\partial \bar{v}}{\partial x}+\frac{\partial \overline{(v')^2}}{\partial x}\right]+\left[\bar{v}\frac{\partial \bar{v}}{\partial y}+\frac{\partial \overline{(v'v')}}{\partial y}\right]+\left[\overline{w}\frac{\partial \bar{v}}{\partial z}+\frac{\partial \overline{v'w'}}{\partial z}\right]= -\frac{1}{\rho}\frac{\partial \bar{p}}{\partial y}+\nu\left(\frac{\partial^2 \bar{v}}{\partial x^2}+\frac{\partial^2 \bar{v}}{\partial y^2}+\frac{\partial^2 \bar{v}}{\partial z^2}\right) \quad (2.2)$$

z momentum equation:

$$\left[\bar{u}\frac{\partial \bar{w}}{\partial x}+\frac{\partial \overline{(w')^2}}{\partial x}\right]+\left[\bar{v}\frac{\partial \bar{w}}{\partial y}+\frac{\partial \overline{(w'v')}}{\partial y}\right]+\left[\overline{w}\frac{\partial \bar{w}}{\partial z}+\frac{\partial \overline{w'w'}}{\partial z}\right]= -\frac{1}{\rho}\frac{\partial \bar{p}}{\partial z}+\nu\left(\frac{\partial^2 \bar{w}}{\partial x^2}+\frac{\partial^2 \bar{w}}{\partial y^2}+\frac{\partial^2 \bar{w}}{\partial z^2}\right) \quad (2.3)$$

Energy equation:

$$\left[\bar{u}\frac{\partial \bar{T}}{\partial x}+\bar{v}\frac{\partial \bar{T}}{\partial y}+\overline{w}\frac{\partial \bar{T}}{\partial z}\right]+\frac{\partial \overline{(u'T')}}{\partial x}+\frac{\partial \overline{(v'T')}}{\partial y}+\frac{\partial \overline{(w'T')}}{\partial z}= \left(\frac{k}{\rho c_p}\right)\left(\frac{\partial^2 \bar{T}}{\partial x^2}+\frac{\partial^2 \bar{T}}{\partial y^2}+\frac{\partial^2 \bar{T}}{\partial z^2}\right) \quad (3)$$

Turbulence kinetic energy equation:

$$\frac{\partial(\rho u k')}{\partial x}+\frac{\partial(\rho v k')}{\partial y}+\frac{\partial(\rho w k')}{\partial z}=\frac{\partial}{\partial x}\left(\frac{\mu_t}{\sigma_k}\frac{\partial k'}{\partial x}\right)+ \frac{\partial}{\partial y}\left(\frac{\mu_t}{\sigma_k}\frac{\partial k'}{\partial y}\right)+\frac{\partial}{\partial z}\left(\frac{\mu_t}{\sigma_k}\frac{\partial k'}{\partial z}\right)+\mu_t\phi-\rho\varepsilon \quad (4)$$

Turbulence viscosity:

$$\mu_t=C_{\mu'}\rho\frac{k'^2}{\varepsilon} \quad (5)$$

At the turbulence model of k-ε in the study employed by Karabulut (2019), when ε displays distribution of turbulence, k′ and ϕ present terms of turbulence kinetic energy and dissipation of viscous, respectively.

Turbulence kinetic energy:

$$k'=\frac{1}{2}\left(\overline{u'^2}+\overline{v'^2}+\overline{w'^2}\right) \quad (6)$$

Viscous dissipation term:

$$\phi=2\mu\left[\left(\frac{\partial u}{\partial x}\right)^2+\left(\frac{\partial v}{\partial y}\right)^2+\left(\frac{\partial w}{\partial z}\right)^2\right]+\mu\left[\left(\frac{\partial v}{\partial x}+\frac{\partial u}{\partial y}\right)^2+ \left(\frac{\partial w}{\partial y}+\frac{\partial v}{\partial z}\right)^2+\left(\frac{\partial u}{\partial z}+\frac{\partial w}{\partial x}\right)^2\right] \quad (7)$$

Turbulence kinetic energy disappearance equation:

$$\frac{\partial(\rho u\varepsilon)}{\partial x}+\frac{\partial(\rho v\varepsilon)}{\partial y}+\frac{\partial(\rho w\varepsilon)}{\partial z}=\frac{\partial}{\partial x}\left(\frac{\mu_t}{\sigma_\varepsilon}\frac{\partial \varepsilon}{\partial x}\right)+\frac{\partial}{\partial y}\left(\frac{\mu_t}{\sigma_\varepsilon}\frac{\partial \varepsilon}{\partial y}\right)+ \frac{\partial}{\partial z}\left(\frac{\mu_t}{\sigma_\varepsilon}\frac{\partial \varepsilon}{\partial z}\right)+C_{1\varepsilon}\mu_t\frac{\varepsilon}{k'}\phi-C_{2\varepsilon}\rho\frac{\varepsilon^2}{k'} \quad (8)$$

C_μ, $C_{1\varepsilon}$, $C_{2\varepsilon}$, σ_k and σ_ε which are model firms are the typical values of default employed in the standard turbulence model of k-ε (Flunet., 2003). The values of these firms were obtained by numerous iterations of data fitting for many turbulent flows.

Re number is computed by the equation given below (Lin and Gao., 2017, Karabulut and Alnak., 2020, Karabulut, 2019).

$$\mathrm{Re}=\frac{V_\infty D_\mathrm{h}}{\nu} \quad (9)$$

D_h is the jet inlet hydraulic diameter (Lin and Gao., 2017, Karabulut and Alnak., 2020, Karabulut, 2019).

$$D_h=\frac{4A_\mathrm{c}}{P} \quad (10)$$

In this equation, A_c and P are the jet inlet cross-sectional area and perimeter lengths, respectively.

The Nu number is defined to be a ratio of the convection heat transfer rate to the conduction heat transfer rate (Welty et. al., 2014).

$$-\mathrm{k}\left(\frac{\partial T}{\partial n}\right)_s=h\Delta T_{lm} \text{ and } Nu=\frac{hL}{k} \quad (11)$$

Here, h is the local heat transfer coefficient on the surface and n is the perpendicular direction to the surface and the local Nu number is calculated as above.

The logarithmic temperature difference between the wall surface of the triangular corrugations and fluid is computed by Liu and Niu (2015).

$$\Delta T_{lm}=\frac{(T_i-T_o)}{ln\left(\frac{T_w-T_i}{T_w-T_o}\right)} \quad (12)$$

where T_i, T_o and T_w are the inlet and outlet temperatures of the fluid and the wall surface temperature of the triangular corrugations, respectively.

Mean heat transfer coefficient (Welty et. al., 2014).

$$h_m = \frac{1}{L}\int_0^L h dx \quad (13)$$

Mean Nu number (Welty et. al., 2014).

$$Nu_m = \frac{h_m L}{k} \quad (14)$$

Pressure drop is calculated with Liu and Niu (2015).

$$\Delta p = \frac{f\rho L}{2D_h} u_m^2 \quad (15)$$

Where Δp is the drop of pressure of the cross-triangular grooved triangular duct between the entry and exit, f is the factor of friction and L is the duct long.

PEC (Performance Evaluation Criterion) number (Akbarzadeh et. al., 2017)

$$PEC = \frac{Nu_{\ channel\ with\ baffles}/Nu_{channel\ without\ baffles}}{(\Delta p_{\ channel\ with\ baffles}/\Delta p_{channel\ without\ baffles})} \quad (16)$$

The dimensionless variable is described as

$$z^* = \frac{z}{L} \quad (17)$$

where z displays the local duct long.

GEOMETRIC DESIGN

Figure 1A illustrates a perspective view of the cross-triangular corrugated duct with rectangular baffles, while Figure 1B shows a channel view depicting boundary conditions and dimensions of the cross-corrugated channel. The dimensions of the triangular cross-grooved duct are specified as follows: length (L) = 70.71 mm, width (W) = 8.165 mm, height of the duct (H) = 7.071 mm, and distance between two rectangular baffles (d) = 8.165 mm. Rectangular baffles are utilized at heights of 0.25H, 0.5H, and 0.75H. The entry velocity range of the air varies from 2.1436 m/s (Re=1000) to 12.8616 m/s (Re=6000). A constant height of 4.0825 mm is maintained for the triangular corrugations. Figure 2 displays the tetrahedral mesh structure for the cross-triangular grooved triangular duct. Based on the duct dimensions reported in the literature, ten rectangular baffles and triangular grooved troughs are present in the lower part of the duct.

This study is conducted under the following assumptions:

a) The flow domain for the cross-triangular grooved triangular duct is three-dimensional (3D), steady, and turbulent.
b) The working fluid used is air, considered to be incompressible.
c) The thermal properties of the air are assumed to be constant throughout the analysis.
d) There is no heat generation within the air flow or on the surfaces of the rectangular baffles.

ASSESSMENT OF THE RESULTS

To assess the influence of grid refinement on the Nusselt number (Nu) of the surfaces within the cross-grooved duct, grid independence tests were conducted for the non-baffled duct across various Reynolds numbers (Re) including 1000, 2000, 3000, and 4000. The results are presented in Table 1. Upon examination of Table 1, it can be observed that 611,037 grid elements are sufficient for achieving grid independence for the non-baffled grooved duct

Tab. 1. Independence of grid test results considering the Nu_m for the grooved duct non-baffle

Mesh Num.	Re=1000 -Nu_m	Re=2000 - Nu_m	Re=3000 - Nu_m	Re=6000 - Nu_m
450571	6.7850	11.285	14.985	23.9356
860452	6.874	11.299	14.9898	23.9402
970002	**6.875**	**11.3**	**14.99**	**23.94**
1152004	6.8754	11.304	14.9954	23.9403

Figures 3a and 3b illustrate the Nusselt number (Nu) values obtained from empirical studies by Scott and Lobato (2003) and computational studies by Liu and Niu (2015), Zhang (2005), Zhang (2005), and Li and Gao (2017). These figures compare the Nu values for apex angles of 60° and 90° in cross-corrugated ducts without baffles, respectively, with the computational results from this study. In Figure 3a, comparisons are made between the computational data from Zhang (2005), Zhang (2005), and Li and Gao (2017), which used the k-ε turbulence model, and the results from this study for a grooved channel with an apex angle of 60° and no baffles. Figure 3b, on the other hand, compares the experimental results from Scott and Lobato (2003) and numerical results from Liu and Niu (2015), Li and Gao (2017), and this study, all of which utilized various turbulence models, for a corrugated duct with an apex angle of 90° without baffles. The maximum deviation observed in this study for Nu is 4.8% compared to numerical results for the 60° apex angle (Figure 3a). However, the differences between the numerical results of this study and the values of the experimental data are within 3.53% for an apex angle of 90° (Figure 3b). The utilization of the k-ε turbulence model demonstrates satisfactory agreement between numerical and experimental results, thus providing a reliable basis for comparative analyses across various rectangular baffle angles and heights.

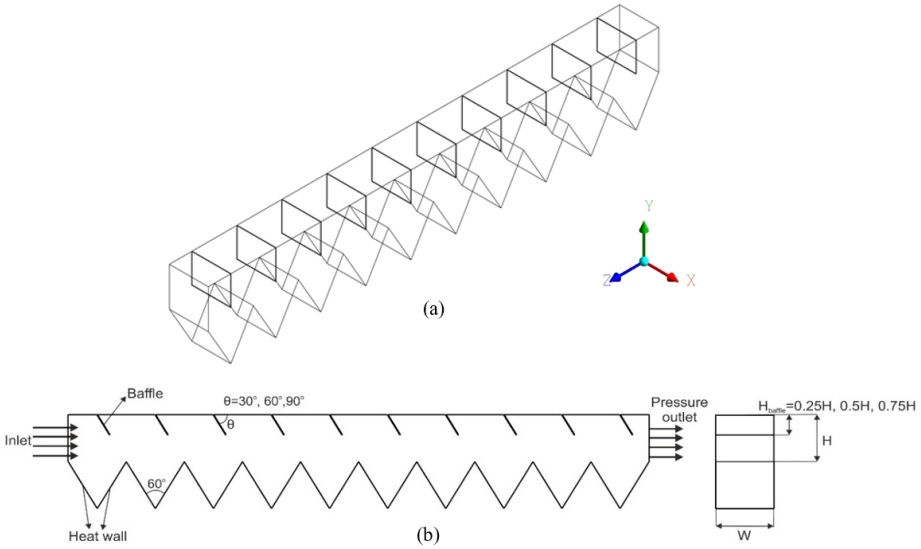

Fig. 1. (a) Cross-triangular corrugated triangular duct perspective view with baffle (b) duct view with dimensions and boundary conditions

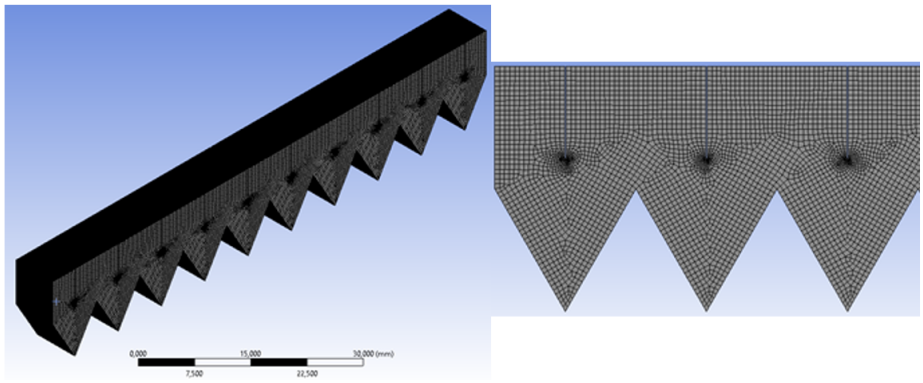

Fig. 2. Cross-triangular corrugated triangular duct mesh structure

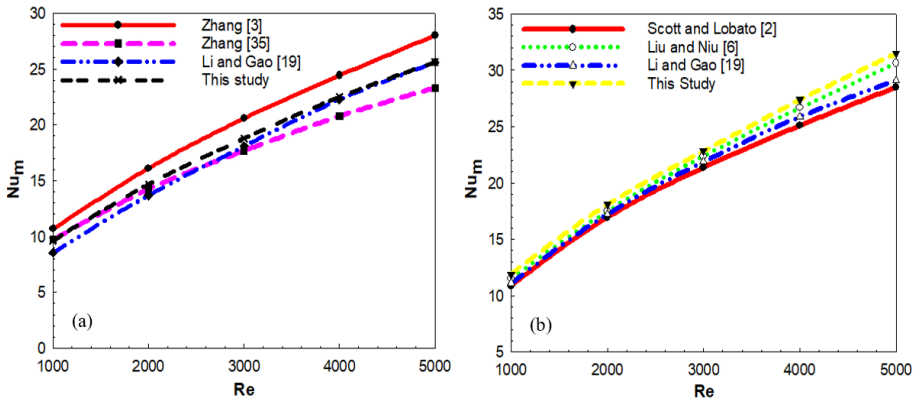

Fig. 3. Mean Nu number (Nu_m) comparing results of the computational and empirical with the outcomes of this work for the apex angles of (a) 60° (b) 90°

Fig. 4. Velocity contour distributions of triangular corrugated rectangular ducts non-baffle and with discrete angles and heights of baffles A-Re=1000 B-Re=6000

Figures 4A and 4B illustrate the velocity contour distributions of rectangular channels with triangular corrugations, both without baffles and with baffles featuring angles of 30°, 60°, and 90°, as well as heights of 0.25H, 0.5H, and 0.75H. In the absence of baffles, the fluid velocity is notably low throughout the channel, including within the triangular corrugations. However, upon the introduction of baffles at the upper section of the rectangular channel, the fluid begins to be directed towards the triangular corrugations. This orientation towards the corrugations becomes more prominent with increasing baffle angle. Additionally,

increasing the baffle height enhances both the direction of flow and turbulence within the fluid and corrugations. As observed in the contour distributions, higher fluid velocities are evident, particularly at baffle angles of 60° and 90°, when using 0.75H height baffles within the duct. At this baffle height (0.75H), under the 90° angled condition, the fluid velocity increases substantially, leading to a jet flow-like scenario due to cross-sectional narrowing in the channel. With the Re number increased to 6000, higher fluid velocity values are observed within the triangular corrugations, as the fluid activity within the duct becomes more pronounced. This increase in Re number results in heightened fluid movement and flow dynamics within the duct.

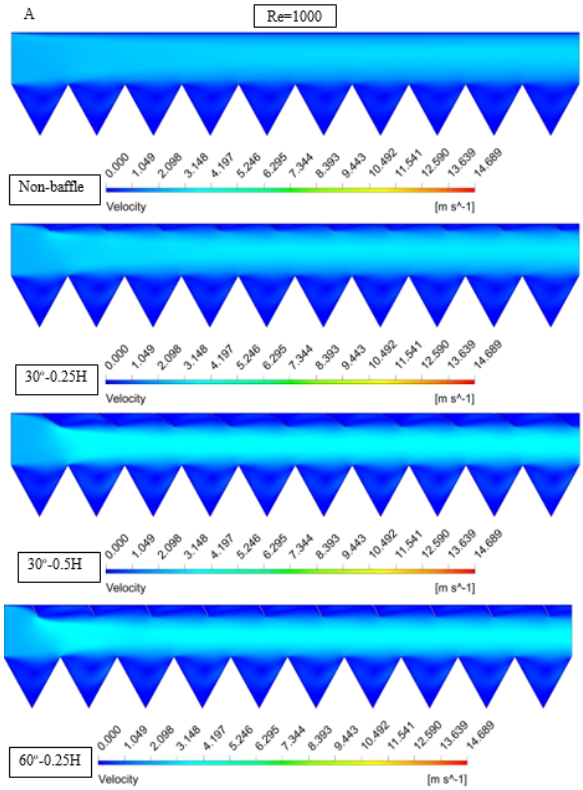

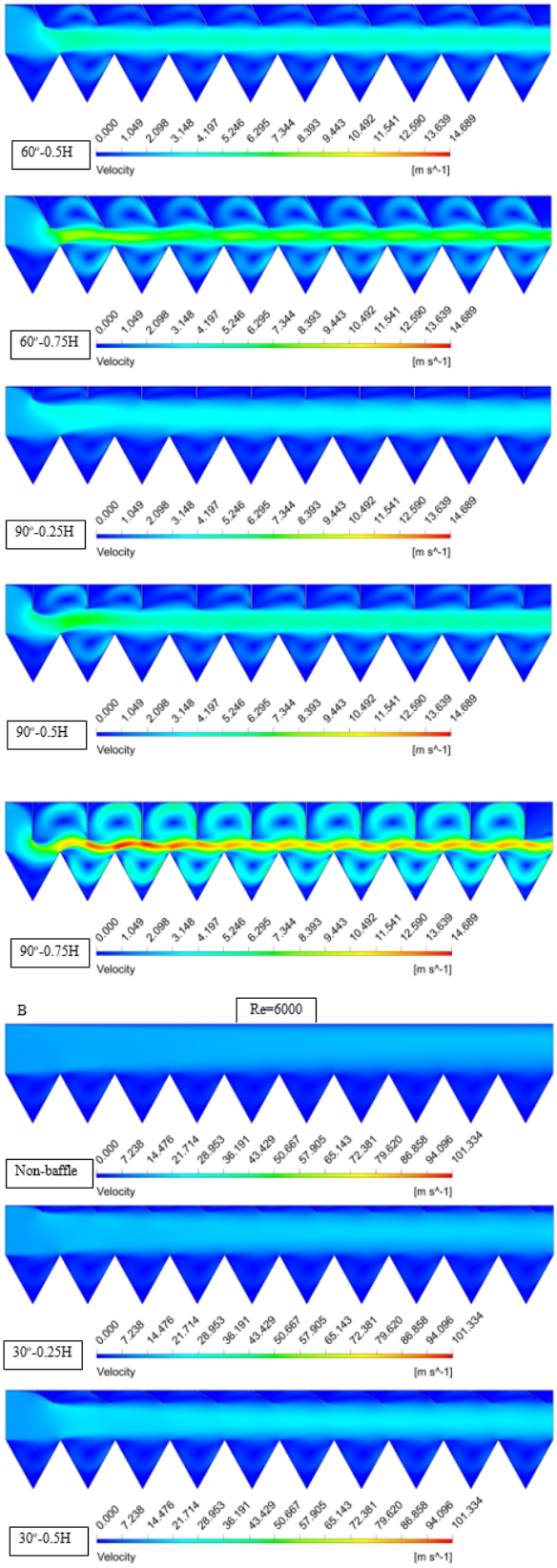

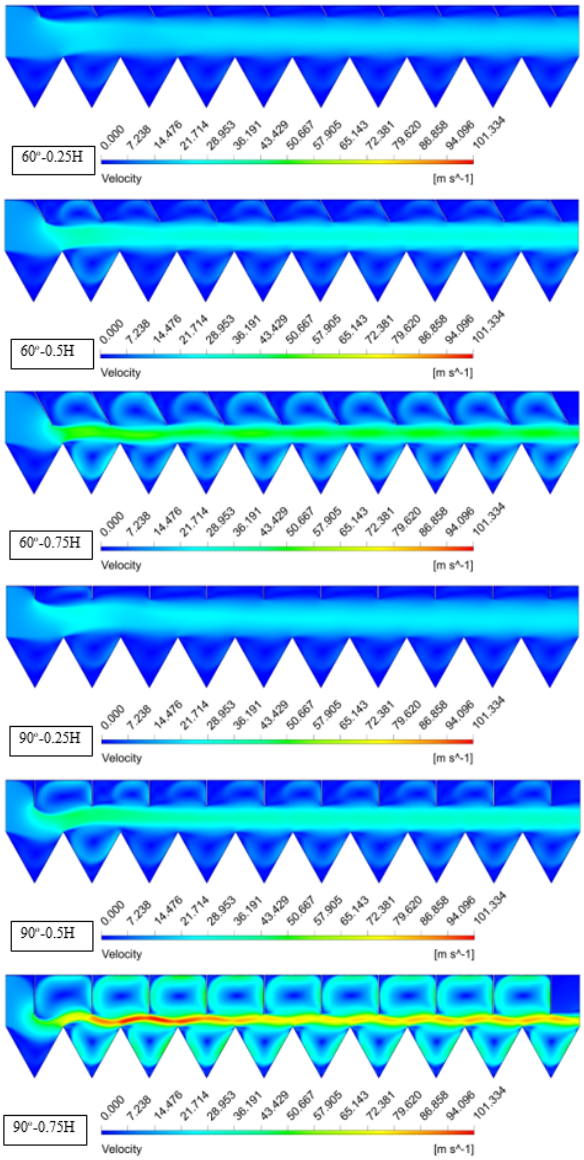

Fig. 4. Velocity contour distributions of triangular corrugated rectangular ducts
non-baffle and with discrete angles and heights of baffles A-Re=1000 B-Re=6000

Figures 5A and 5B depict the temperature contour distributions of rectangular ducts with triangular corrugations, both without baffles and with baffle angles of 30°, 60°, and 90°, as well as heights of 0.25H, 0.5H, and 0.75H, at Reynolds numbers (Re) of 1000 and 6000, respectively. In the absence of baffles, temperatures are notably high throughout the channels and within the triangular corrugations, indicating a need for cooling. At the peaks of the triangular corrugations, temperatures reach their highest values. Upon the addition of baffles to the channels, the fluid is directed towards these corrugations, facilitating cooling and reducing their temperature. Consequently, towards the end of the duct, the fluid within the channel and between the baffles experiences heating, leading to increased temperatures. With increasing baffle angle and height, the orientation towards the corrugations improves, enhancing heat transfer. This effect is particularly pronounced at a height of 0.75H for Re=6000 and at baffle angles of 60° and 90°, where the reduction in temperature is most evident. Overall, using baffles enhances heat transfer efficiency and reduces temperature within the duct

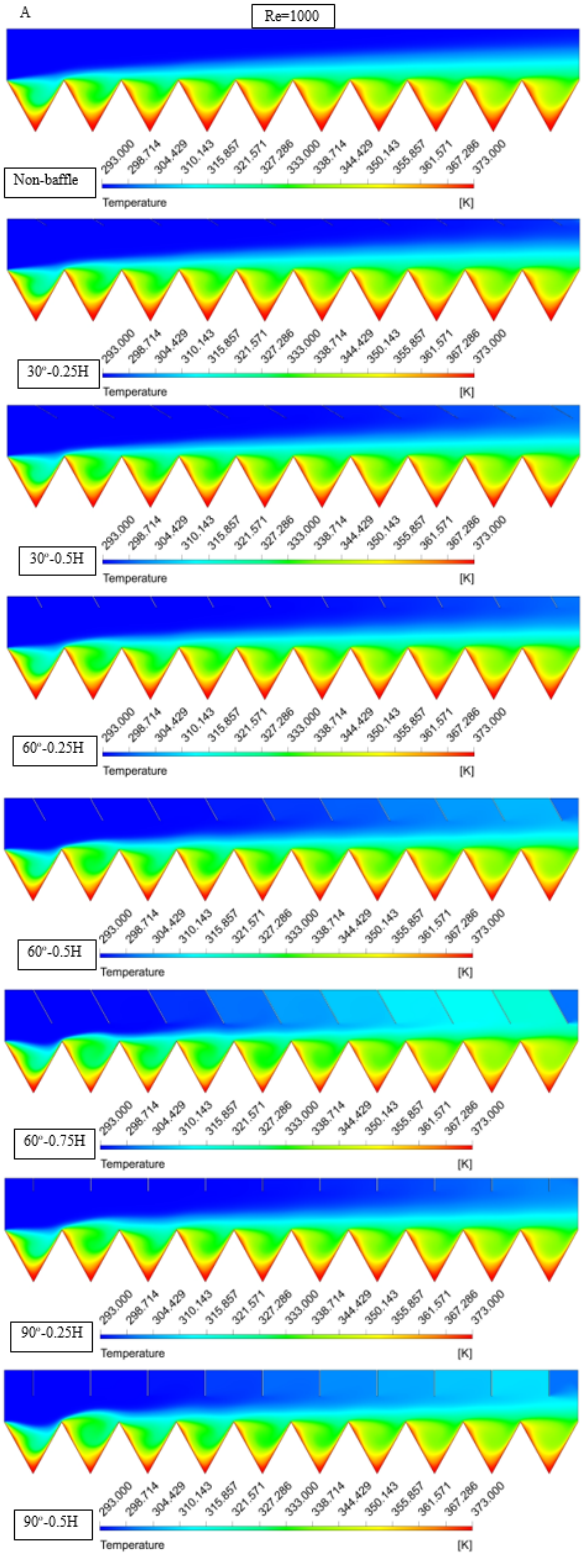

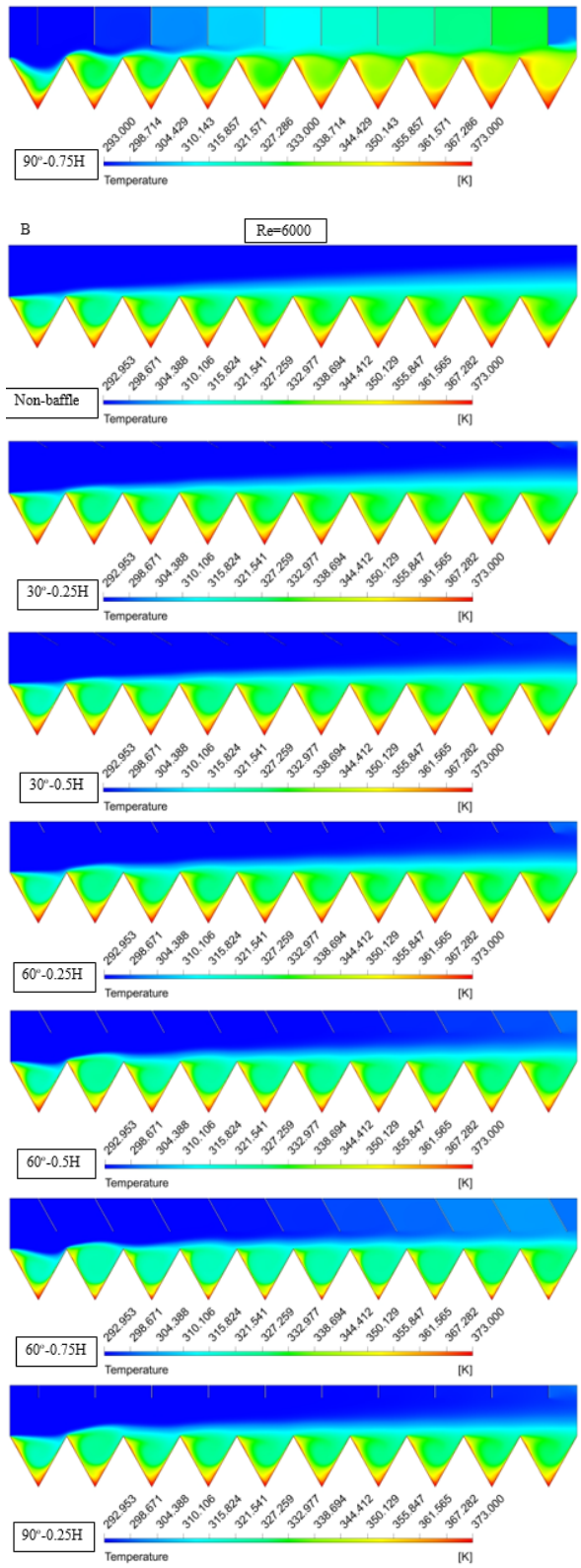

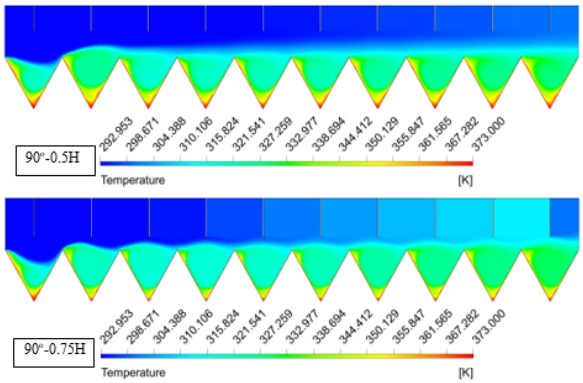

Fig. 5. Contour distributions of temperature of triangular grooved rectangular ducts
non-baffle and with discrete angles and heights of baffles A-Re=1000 B-Re=6000

Figure 6 illustrates the temperature variations along the rectangular channels with triangular corrugations, categorized by Reynolds numbers, and different baffle angles and heights. In the case of non-baffles (Figure 6a), temperatures of the fluids decrease as the Reynolds number increases, indicating enhanced cooling efficiency with higher fluid velocities. However, when baffles are introduced, temperature variations become more complex. Figures 6b to 6i represent the temperature variations for different baffle configurations, including various baffle angles and heights. It is observed that temperature values tend to increase with higher baffle angles and heights. This is because the baffles direct the flow towards the triangular corrugations, resulting in increased heat transfer and thus higher temperatures. Interestingly, fluctuations in temperature, particularly at the duct entrances, are observed depending on the angle and height setups of the baffles. However, in the channel arrangement with a 90° angle and 0.75H baffle height, temperatures reach their highest values more periodically and regularly compared to other channels. This suggests that this particular baffle configuration may offer more efficient and consistent heat transfer performance.

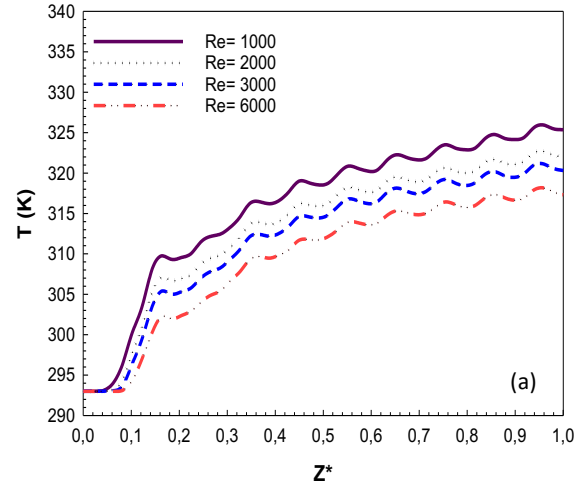
Re= 1000
Re= 2000
Re= 3000
Re= 6000
T (K)
Z*
(a)

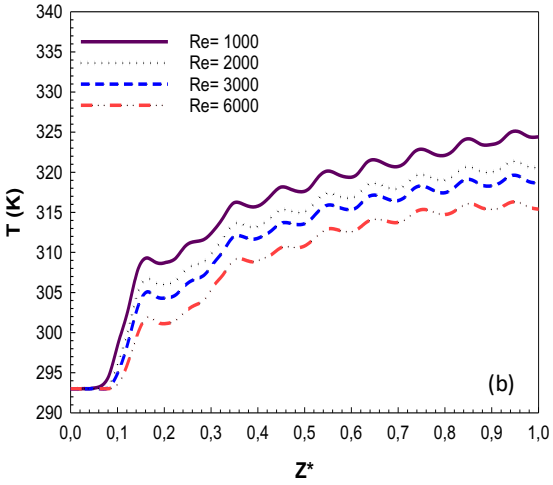
Re= 1000
Re= 2000
Re= 3000
Re= 6000
T (K)
Z*
(b)

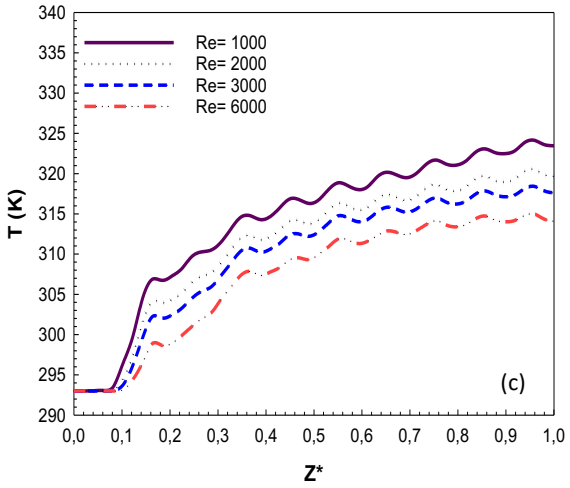
Re= 1000
Re= 2000
Re= 3000
Re= 6000
T (K)
Z*
(c)

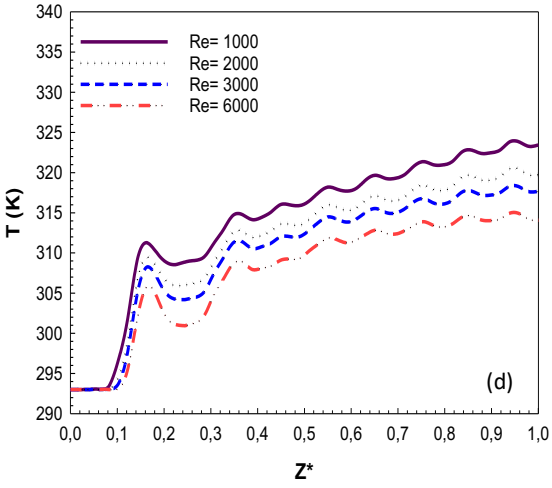
Re= 1000
Re= 2000
Re= 3000
Re= 6000
T (K)
Z*
(d)

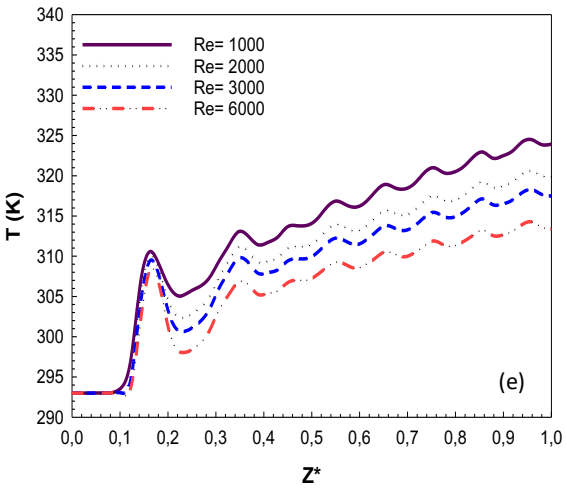
Re= 1000
Re= 2000
Re= 3000
Re= 6000
T (K)
Z*
(e)

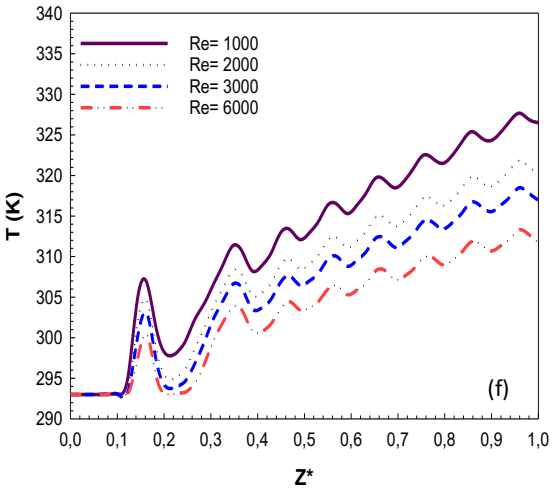
Re= 1000
Re= 2000
Re= 3000
Re= 6000
T (K)
Z*
(f)

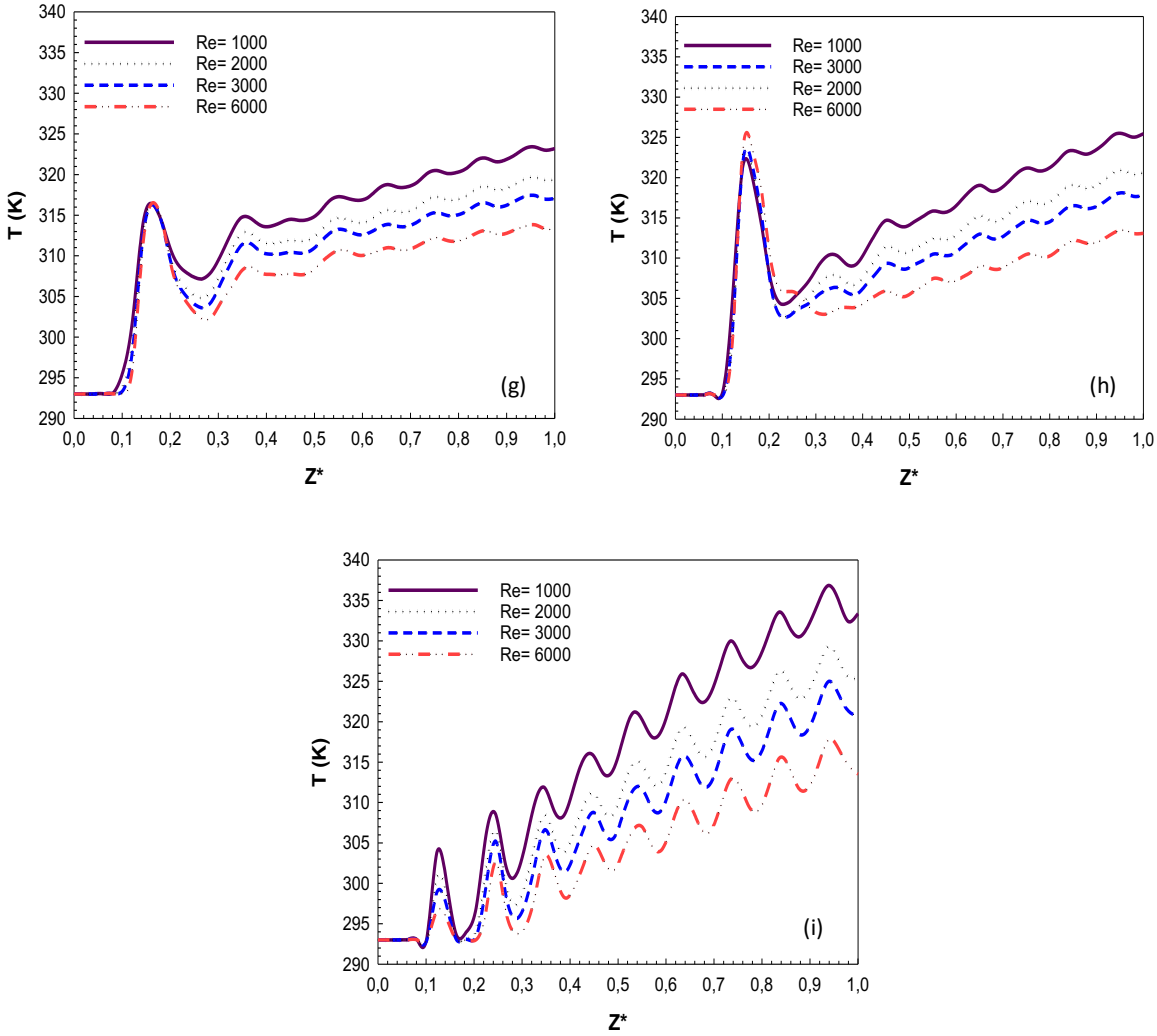

Fig. 6. Fluid temperature value variations of triangular corrugated rectangular ducts for the non-baffle duct (a) and ducts with discrete baffle angles and heights (b) 30º-0.25H (c) 30º-0.5H (d) 60º-0.25H (e) 60º-0.5H (f) 60º-0.75H (g) 90º-0.25H (h) 90º-0.5H (i) 90º-0.75H

Figure 7 displays the variations in mean Nusselt number (Num) versus different Reynolds numbers (Re) for rectangular channels with triangular corrugations, both without baffles and with rectangular baffles featuring angles of 30°, 60°, and 90°, as well as heights of (a) 0.25H, (b) 0.5H, and (c) 0.75H, respectively. Observations from the figure reveal that Nu values increase with higher heat transfer rates, corresponding to the increase in Reynolds number. This trend is consistent across all baffle configurations. Interestingly, the maximum Nu value is consistently achieved for all baffle heights at a baffle angle of 90°. This indicates that the fluid flow experiences more intense vortex movements due to turbulence created within the fluid at this particular baffle angle value. Moreover, the highest Nu value is observed at a baffle angle of 90° and a baffle height of 0.75H. Specifically, at this configuration, the Nu value increases by 197.56% at Re=6000 compared to the Nu value at a baffle height of 0.25H for the same Reynolds number. This substantial increase in Nu highlights the significant enhancement in heat transfer efficiency achieved by employing the 90° angle and 0.75H baffle height configuration.

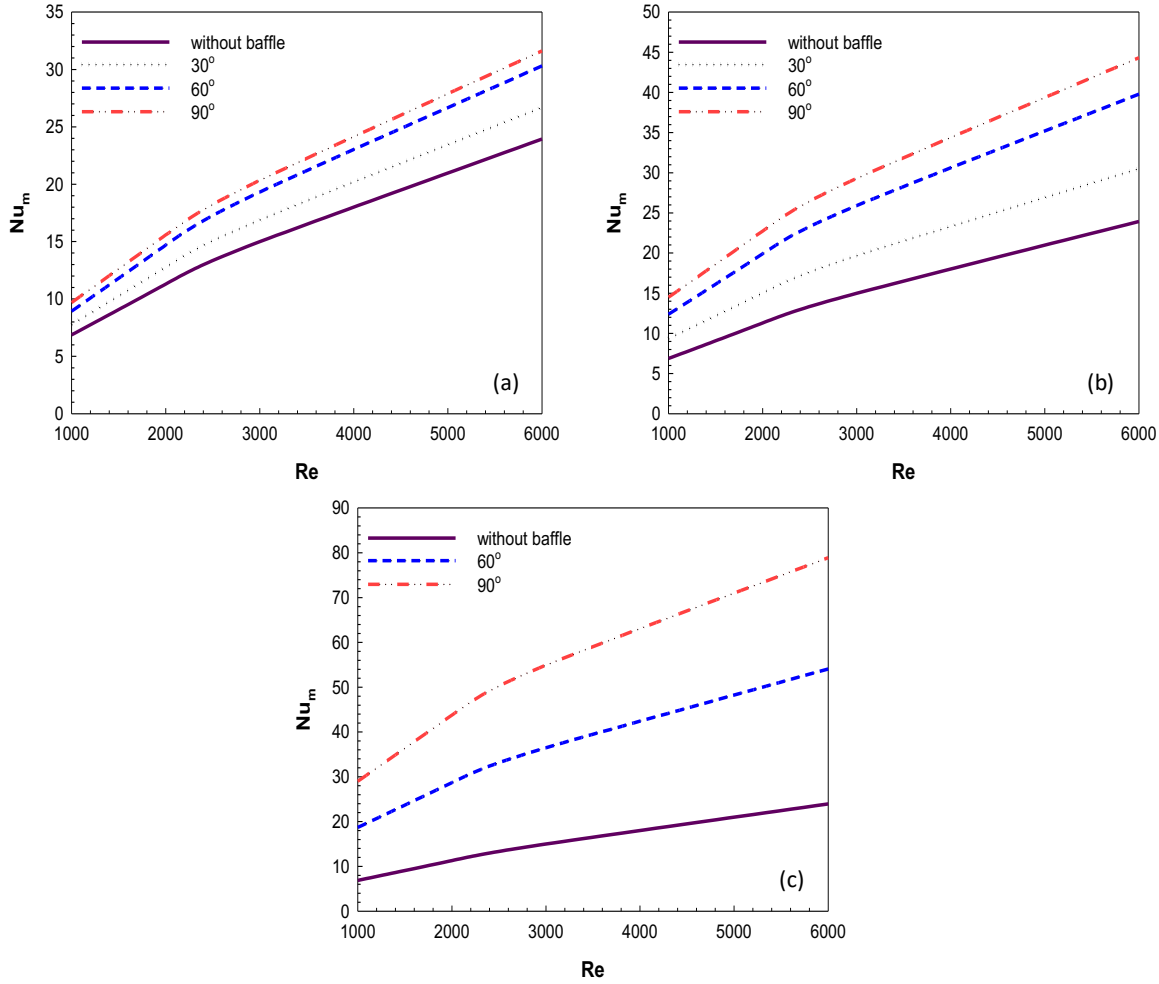

Fig. 7. Mean Nu number (Nu_m) variations of triangular corrugated rectangular ducts for the non-baffle and with baffle-angled for the baffle height of (a) 0.25H (b) 0.5H (c) 0.75H

In Figure 8, temperature variations of the fluid at the outlet of the rectangular channel with triangular corrugations are depicted, considering different baffle angles (30°, 60°, and 90°) and height arrangements of (a) 0.25H, (b) 0.5H, and (c) 0.75H, respectively. Observations from the figure reveal that the temperature values of the fluid at the exit of the duct decrease with increasing Reynolds number. This decrease is attributed to the enhanced heat transfer efficiency associated with higher fluid velocities. Moreover, temperature values increase as the baffle angle and height are increased. This increase in temperature is due to the improved heat transfer achieved by directing the flow towards the triangular corrugations through the use of baffles. Comparing with the non-baffled situation, the highest temperature values are obtained for the duct with a 90° baffle angle and 0.75H height. This configuration enhances heat transfer efficiency to the extent that it results in the highest temperature values at the duct outlet.

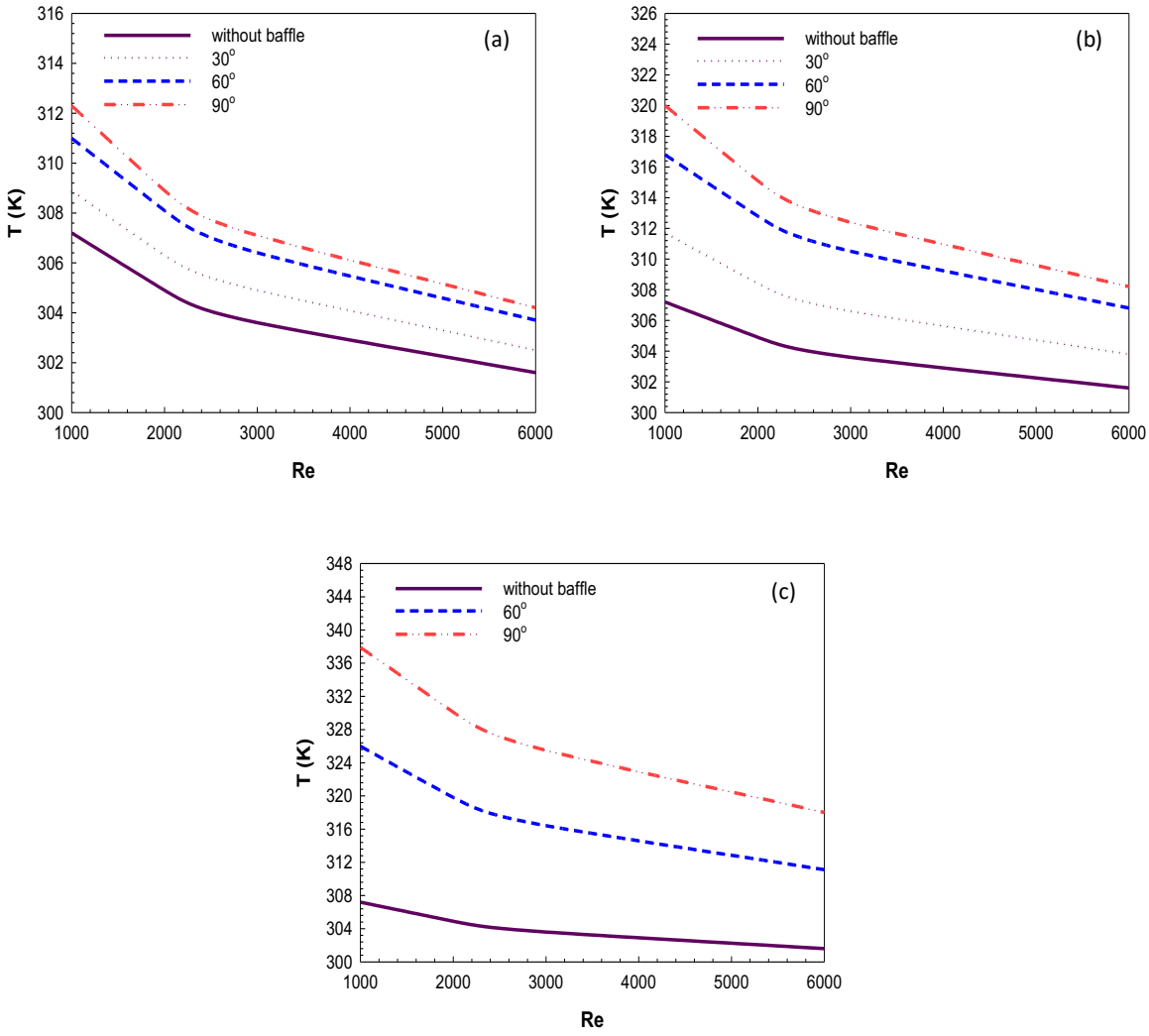

Fig. 8. Fluid outlet temperature variations of triangular corrugated rectangular ducts for the non-baffle and with baffle-angled for the baffle height of (a) 0.25H (b) 0.5H (c) 0.75H

In Figure 9, variations of the Performance Evaluation Criterion (PEC) for rectangular channels with triangular corrugations are depicted as a function of Reynolds number (Re), considering different baffle angles (30°, 60°, and 90°) and heights of (a) 0.25H, (b) 0.5H, and (c) 0.75H, respectively. PEC is a thermal-hydraulic performance factor, representing the ratio of the mean Nusselt number (Nu) enhancement to the increase in pressure drop (Δp) in the baffled state compared to the non-baffled state. Observations from the figure indicate that the PEC number decreases with increasing baffle angle, height, and Reynolds number. This decrease occurs because the enhancement in pressure drop (Δp) outweighs the increase in Nu, resulting in a lower PEC value. For example, at Re=1000, the PEC number is 84.50% higher at a baffle height of 0.25H and a baffle angle of 30° compared to the 90° angled condition. This suggests that the 30° baffle angle configuration at a height of 0.25H offers better thermal-hydraulic performance, as it achieves a higher PEC number due to a more favourable effect between Nu improvement and pressure drop increase. Although the PEC value decreases with the increase in the baffle height and angle, the fact that relatively higher PEC number values are obtained at low height and angle values shows that the investigated geometries have potential to be used in heat transfer applications in order to use energy more efficiently and economically, considering the increase in heat transfer performance achieved. Similar results were obtained in the studies in the literature (Li and Gao (2017), Feng et al. (2022) and Liang et al. (2019)), and with the addition of baffles to the channels, a significant pressure drop and friction factor increase were observed despite the increase in the Nu number.

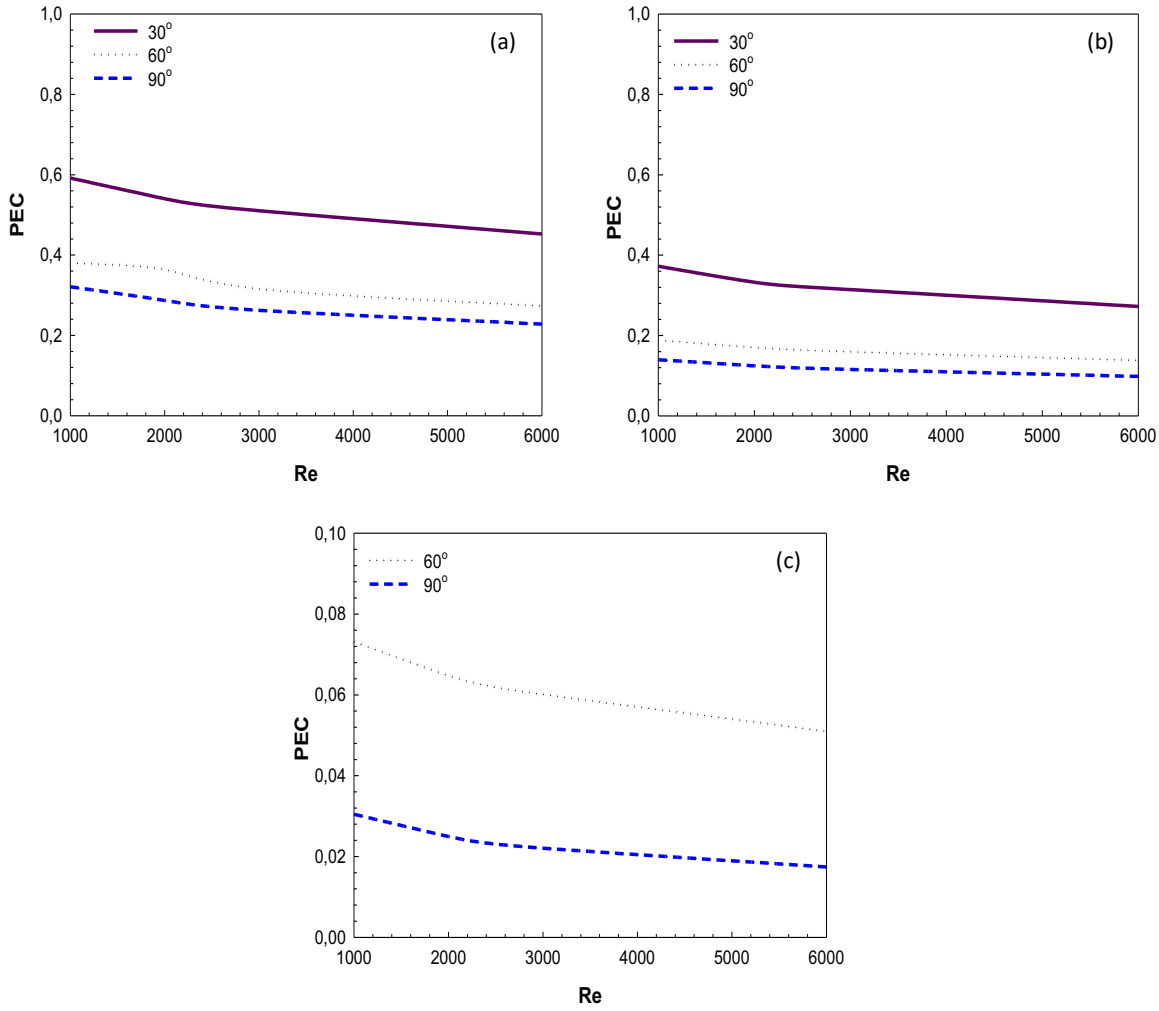

Fig. 9. Performance Evaluation Criterion (PEC) number variations of triangular corrugated rectangular ducts for the without baffle and with baffle-angled for the baffle height of (a) 0.25H (b) 0.5H (c) 0.75H

CONCLUSIONS

This study comprehensively investigates the effects of various rectangular baffle angles and heights in rectangular channels with triangular corrugations on several parameters including heat transfer (Num), fluid outlet temperature, and the performance evaluation criterion (PEC) taking into consideration of pressure drop. The findings are summarized as follows:

Introduction of baffles into the rectangular channel redirects the fluid flow towards the triangular corrugations, increasing the flow velocity and turbulence within the fluid and corrugations. Particularly, at higher baffle angles and heights, such as 60° and 90° with a 0.75H height, the fluid velocity increases significantly, resembling a jet flow-like situation.

Baffles intensify turbulence within the duct, enhancing heat transfer. This increase in turbulence intensity is particularly pronounced at the baffle tips and corrugation tops, and it penetrates deeper into the corrugations and baffle spaces with higher baffle angles and heights.

Temperature decreases along the channel with increasing Reynolds number but increases with higher baffle angles and heights. However, temperature fluctuations, especially at duct entrances, are observed based on the baffle angle and height configurations. Channels with a 90° baffle angle and 0.75H height exhibit more periodic and regular temperature peaks.

Mean Nusselt number (Num) increases with higher Reynolds numbers, with the maximum Num achieved at a baffle angle of 90°. The highest Num value is observed at a 90° angle and 0.75H baffle height, with a 197.56% increase compared to a 0.25H baffle height at Re=6000.

Outlet temperature increases with higher heat transfer improvement resulting from increased baffle angle and height. The highest temperature values are obtained for channels with a 90° baffle angle and 0.75H height, particularly in non-baffled situations.

Performance Evaluation Criterion (PEC) decreases with increasing baffle angle, height, and Reynolds number due to the greater increase in pressure drop compared to the increase in Num. Specifically, for Re=1000, PEC is 84.50% higher at a 0.25H baffle height and 30° baffle angle compared to a 90° angle condition.

Overall, this study provides valuable insights into the thermal-hydraulic performance of rectangular channels with triangular corrugations and demonstrates the significant impact of baffle angle and height configurations on various performance parameters.

NOMENCLATURE

A_c	Jet inlet cross section, [m^2]
H	Channel height, [m]
L	Channel lenght, [m]
W	Channel width, [m]
D_h	Hydraulic diameter of the channel, [m]
h	Local convective heat transfer coefficient, [$Wm^{-2}K^{-1}$]
k	Thermal conductivity, [$Wm^{-1}K^{-1}$]
V	Fluid velocity in the channel entry, [ms^{-1}]
c_p	Specific heat capacity of the fluid, [$Jkg^{-1}K^{-1}$]
P	Jet inlet cross section perimeter length,[m]
p	Pressure, [Nm^{-2}]
T	Temperature, [K]
u, v, w	Velocity components of x,y,z directions, [ms^{-1}]
u',v',w'	Fluctuating velocity components in x,y,z directions, [ms^{-1}]
$\overline{u}, \overline{v}, \overline{w}$	Mean velocities in coordinates, [ms^{-1}]
Re	Reynolds number [$=V_\infty D_h/v$]
Nu	Local Nusselt number [=hL/k]

Greek Symbols

μ	Dynamic viscosity, [$kgs^{-1}m^{-1}$]
μ_t	Turbulent viscosity, [$kgs^{-1}m^{-1}$]
υ	Kinematic viscosity, [m^2s^{-1}]
ρ	Density, kgm^{-3}
ϕ	Viscous dissipation term, [m^2s^{-3}]
k'	Turbulance kinetic energy, [m^2s^{-2}]
ε	Turbulent dissipation rate, [m^2s^{-3}]
φ	Rectangular baffle angle, [°]

Subscripts

s	Surface
sm	Surface mean
∞	Fluid
m	Mean

REFERENCES

Ajeel R.K., Salim W.S.-I.W., Hasnan K. Influences of geometrical parameters on the heat transfer characteristics through symmetry trapezoidal-corrugated channel using SiO_2-water nanofluid, Int. Comm. Heat Mass Transf. 101, 1–9, 2019.

Ajeel R.K., Salim W.S.-I.W., Hasnan K. Experimental and numerical investigations of convection heat transfer in corrugated channels using alumina nanofluid under a turbulent flow regime, Chem. Eng. Res. Des. 148, 202-217, 2019.

Ajeel R.K., Salim W.S.-I.W., Hasnan K. An experimental investigation of thermal-hydraulic performance of silica nanofluid in corrugated channels, Ad. Powder Technol. 30, 2262–2275, 2019.

Alnak D.E. Thermohydraulic performance study of different square baffle angles in cross-corrugated channel, Journal of Energy Storage, 28, 101295, 2020.

Aslan, E., Taymaz, I., Cakır, K., Eker Kahvecı, E. Numerical and experimental investigation of tube bundle heat exchanger arrangement effect on heat transfer performance in turbulent flows, J. of Thermal Science and Technology 43 (2), 175-190, 2023.

Akbarzadeh, M., Rashidi, S., Esfahani, J. A. Influences of corrugation profiles on entropy generation, heat transfer, pressure drop, and performance in a wavy channel, Appl. Therm. Eng. 1 (2017) 278–291.

Feng C.N., Liang C.H., Li Z.X. Friction factor and heat transfer evaluation of cross-corrugated triangular flow channels with trapezoidal baffles, Energy&Buildings, 257, 111816, 2022.

FLUENT User's Guide, Fluent Inc. Lebanon, Netherland, 2003.

Guo-Yan Z., Shan-Tung T., Hu-Gen M. Numerical and experimental study on the heat transfer and pressure drop of compact cross-corrugated recuperators, J. Heat Transf. 136, 071801, 2014.

Karabulut, K. Investigation of heat transfer improvements of graphene oxide-water and diamond-water nanofluids in cross-flow-impinging jet flow channels having fin, J. of Thermal Science and Technology 43 (1), 11-30, 2023.

Karabulut K. Heat transfer increment study taking into consideration fin lengths for CuO-water nanofluid in cross flow-impinging jet flow channels, Thermal Science, 27 (6A), 4345-4360, (2023).

Karabulut, K., Alnak, Y. A study on microchip cooling performance increment by using air jet impingement with one and double rows. Proceedings of the Institution of Mechanical Engineers, Part E: Journal of Process Mechanical Engineering, 0 (0), 2023.

Karabulut, K., Alnak, D.E. Study of cooling of the varied designed warmed surfaces with an air jet impingement, Pamukkale Univ. J. Eng. Sci. 26 (1), 88-98, 2020.

Karabulut, K. Heat transfer improvement study of electronic component surfaces using air jet impingement, J. Comput. Electron 18, 1259-1271, 2019.

Krishnan E.N., Ramin H., Guruabalan A., Simonson C.J. Experimental investigation on thermo-hydraulic performance of triangular cross-corrugated flow passages, Int. Commun. Heat Mass Tran. 122, 105160, 2021.

Liang C.H., Feng C.N., Lei T.Y., Li Z.X. Numerical studies on the effect of the baffle on the heat transfer and flow in cross-corrugated triangular ducts, IOP Conf. Series: Earth and Environmental Science, 238, 012086, 2019.

Liu X.P., Niu J.L. Effects of geometrical parameters on the thermohydraulic characteristics of periodic cross-corrugated channels, Int. J. Heat Mass Tran. 84, 542–549, 2015.

Li Z.X., Zhong T.S., Niu J.L., Xiao F., Zhang L.Z. Conjugate heat and mass transfer in a total heat exchanger with cross-corrugated triangular ducts and one-step made asymmetric membranes, Int. J. Heat Mass Tran. 84, 390–400, 2015.

Li Z-X., Sun S-Q., Wang C., Liang C.H., Zeng S., Zhong T., Hu W-P., Feng C-N. The effect of trapezoidal baffles on heat and flow characteristics of a cross-corrugated triangular duct, Case Studies in Thermal Engineering 33, 101903, 2022.

Li Z., Gao Y. Numerical study of turbulent flow and heat transfer in cross-corrugated triangular ducts with delta-shaped baffles, Int. J. Heat Mass Transf. 108, 658–670, 2017.

Liang C.H., Feng C.N., Lei T.Y., Li Z.X. Numerical studies on the effect of baffle on the heat transfer and flow in cross-corrugated triangular ducts, IOP Conf. Series: Earth and Environmental Science, 238, 012086, 2019.

Muley A., Manglik R.M. Experimental study of turbulent flow heat transfer and pressure drop in a plate heat exchanger with Chevron plates, ASME J. Heat Transfer, 121, 110–117, 1999.

Saha S.K., Khan A.H. Numerical study on the effect of corrugation angle on thermal performance of cross corrugated plate heat exchangers, Therm. Sci. Eng. Prog. 20, 100711, 2020.

Saim R., Bouchenafa R., Benzenine H., Oztöp H.F., Al-Salem K., Abboudi S. A computational work on turbulent flow and heat transfer in a channel fitted with inclined baffles, Heat Mass Trans 49, 761–774, 2013.

Scott K., Lobato J. Mass transport in cross-corrugated membranes and influence of TiO_2 for separation processes, Industrial&Engineering Chemistry Research, 42 (22), 5697-5701, 2003.

Wang S.J., Mujumdar A.S. A Comparative study of five low Reynolds number k-ε models for impingement heat transfer, Applied Thermal Engineering, 25, 31-44, 2005.

Welty, J., Rorrer, G.L., Foster, D.G. revised 6th edition, Fundamentals of Momentum, Heat, and Mass Transfer 768 Wiley, United States, 2014 ISBN: 978-1-118-94746-3.

Yıldızeli, A., Cadırcı, S. Numerical investıgatıon of plate coolıng using multiple impinging jets in different alignments, J. of Thermal Science and Technology 43 (1), 1-10, 2023.

Zhang L. Numerical study of periodically fully developed flow and heat transfer in cross-corrugated triangular channels in transitional flow regime, Numerical Heat Transfer Part A: Applications, 48 (4), 387-405, 2005.

Zhang L.Z. A reliability-based optimization of membrane-type total heat exchangers under uncertain design parameters, Energy, 101, 390-401, 2016.

Zhang L.Z. Turbulent three-dimensional air flow and heat transfer in a cross-corrugated triangular duct, J. Heat Tran. 127, 1151–1158, 2005.

Zhang L.Z. Numerical study of periodically fully developed flow and heat transfer in cross-corrugated triangular channels in transitional flow regime, Numer. Heat Tran. 48, 387–405, 2005.

Zhang L.Z., Chen Z.Y. Convective heat transfer in cross-corrugated triangular ducts under uniform heat flux boundary conditions, Int. J. Heat Mass Tran. 54, 597–605, 2011.

Zhang, L.Z. Convective mass transport in cross-corrugated membrane exchangers, Journal of Membrane Science 260, 75–83, 2005.

Zimmerer C., Gshwind P., Gaiser G., Kottke V. Comparison of heat and mass transfer in different heat exchanger geometries with corrugated walls, Exp. Therm. Fluid Sci. 26, 269–273, 2002.

Statements&Declarations

Competing Interests and Funding

The author has no relevant financial or non-financial interests to disclose.

Author Contribution

The author contributed to the study's conception and design. Material preparation, data collection and analysis were performed by Yeliz ALNAK. The first draft of the manuscript was written by Yeliz ALNAK and the author commented on previous versions of the manuscript. The author read and approved the final manuscript.

Data Availability

The data that support the findings of this study are available from the corresponding author upon reasonable request.

Author information

Yeliz Alnak received her bachelor's degree from Ataturk University of machine engineering, Erzurum, Turkiye, in 2003. She is her master's degrees from Sivas Cumhuriyet University, machine engineering, Sivas, Turkiye, in 2007. She is her Ph.D. from Firat University, in machine train-ing, Elazığ, Turkiye, in 2020. She is a doctoral faculty member at Sivas Cumhuriyet University Faculty of Technology. Her research interests including energy, CFD, Ansys, fluid flow.